Synthesis and Characterization of Conductive Polypyrrole/Montmorillonite Nanocomposites via One-pot Emulsion Polymerization

S. J. Peighambardoust,[1,2] *Behzad Pourabbas**[1,2]

Summary: A series of electrically conductive polypyrrole/clay nanocomposites were synthesized in this work by using one-pot emulsion oxidative polymerization of pyrrole in the presence of unmodified clay and using DBSNa as the surfactant. The effect of surfactant on the morphological and electrical properties of PPy also were investigated and discussed in some extent. Electrical conductivity of the samples was measured by using samples in which the conductive materials was sandwiched between two Ni electrodes at room temperature. PPy/MMT nanocomposites were characterized by using XRD, TEM, TGA and DSC means of investigation. Intercalated structures were determined for the nanocomposites as confirmed by XRD and TEM studies. Electrical conductivity of the nanocomposites was measured to be dependent to the clay content, and the methods of preparation. Measurement also showed that polymerization of pyrrole monomers pre-intercalated between the clay gallery spaces of the clay led to higher conductivity for the nanocomposite in the same level of clay content. Thermal property measurements showed a lower thermal decomposition rate for the PPy/MMT nanocomposites with respect to the PPy.

Keywords: clay; conductive nanocomposites; electrical conductivity; polypyrrole

1. Introduction

Inherently conductive polymers are a class of polymeric materials with conjugated unsaturated bonds at the main chains. They have been proposed for several applications in electrical and electronic industries such as molecular electronic devices,[1] solid-state electrodes for battreis,[2] solid-electrolyte capacitors,[3] light emitting diodes,[4] electromagnetic interference (EMI) shielding materials,[5] ion-sensors[6–7] and corrosion protection.[8]

Polypyrrole (PPy) is among the most studied conducting polymers because of its high electrical conductivity, environmental stability and relatively ease of synthesis.[9].

PPy can be prepared by electrochemical[10–12] or chemical[13,14] oxidation of pyrrole monomer in various organic solvents and/or in aqueous media. In chemical oxidative polymerization, pyrrole monomers become oxidized by using an oxidizing agent such as ferric chloride,[13,15] ferric perchlorate[16] and ammonium peroxydisulfate.[17–18] PPy can also be synthesized in the form of stable colloids by using polymeric stabilizers or surfactants.[19–21] In this case, the effect of the surfactant molecules is that firstly, they provide requirements for the polymerization reaction to proceed via the emulsion[22–23] or inverse emulsion[24–26] pathway. Secondly, they lead to an improvement in properties such as conductivity, stability, solubility in organic solvents, and the processibility.[27] Some advantageous are reported for PPy samples synthesized in the presence of an anionic surfactant.[9] These advantages are mentioned to be improved stability toward

[1] 1-Nanostructured Materials Research Center, Sahand University of Technology, Tabriz 51335-1996, Iran
[2] 2- Polymeric Materials Research Center, Sahand University of Technology, Tabriz 51335-1996, Iran
Tel: (+)98-411-4249610, Fax:(+)98-411-4249610
E-mail: pourabas@sut.ac.ir

deprotonation, better thermooxidative and thermal stability,[9] improved electrical parameters,[27] morphology that is more compact and reduced size PPy globules.[28] Higher solubility is also reported that can be achieved for PPy in the case of using surfactant in the synthesis.[29] It was also reported that the mentioned advantages can be achieved only in the case of using anionic surfactants and cationic or neutral surfactants were reported to be ineffective.[9] So far, the anionic surfactants in the form of free acid or salt have been the mostly used stabilizers for these purposes.[27] Dodecyl benzene sulfonic acid[30–36] or its substituted derivatives,[22,37–41] sodium dodecyl benzene sulfonate[28,42–46] and sodium dodecyl sulfate[25–26] are among the mostly used surfactants in the form of free acid or salts.

In recent years, polymer/layered silicate (PLS) nanocomposites have been received to a great level of interests because of their superior properties and potential applications as new materials.[47] Therefore, several types of PLSs materials have been prepared by using clay minerals as the layered silicate and many different polymeric systems as the matrices.[47] Electrically conductive nanocomposites[48–49] including PPy/clay nanocomposites[8,50–55] have also been prepared by intercalation of the polymeric chains between the layers of the clay fillers. Among various clay materials, montmorillonite (MMT), whose lamellae are constructed from an octahedral silica sheets, exhibit a net negative charge on the lamellae surface, and causes it to adsorb cation such as Na^+ or Ca^+.[56] Negatively charged layers of MMT act as polyanion and facilitate insertion of the positively charged electrically conductive polymer chains.

It has been reported that incorporation of clay layers in PPy matrix bring with changes in chemical, physical and mechanical properties of the nanocomposite in comparison to the pristine PPy. Enhance in corrosion protection effect, slightly higher decomposition temperature and significant increase in T_g are among the reported advantages for PPy/MMT reported by previous researchers.[57] From the other hand, decrease in electrical conductivity due to insertion of none-conductive layered clay into the matrix of PPy and decreased conjugated length in PPy chains indicating the structurally restricted polymerization are other reported changes in properties for PPy/MMT nanocomposites.[57]

This work has a new approach to the synthesis of electrically conducting PPy/MMT nanocomposites. In this work, a series of PPy/MMT nanocomposites have been prepared by emulsion polymerization method using DBSNa as the surfactant and $FeCl_3 \cdot H_2O$ or $Fe_2(SO_4)_3$ as the oxidizing agent. The effect of oxidizing agent and polymerization method, also the effect of clay content has been investigated on the PPy and PPy/MMT nanocomposites by XRD, SEM, TEM, TGA and DSC methods of investigation. The electrical property of the samples also was investigated at room temperature by using test samples prepared as is described in the text.

2. Experimental Part

2.1 Materials

Pyrrole monomer (Merck) was purified by distillation under reduced pressure before use. The oxidizing agents, ferric chloride ($FeCl_3 \cdot 6H_2O$) and ferric sulfate ($Fe_2(SO_4)_3$) were purchased from Merck and Fluka respectively. Sodium dodecyl benzene sulfonate (DBSNa) was purchased from Fluka. The layered silicate in the present work was Montmorillonite (MMT) K10 from the Aldrich chemical company. All the other ordinary chemicals used in this work were laboratory grades mainly obtained by Merck or Fluka chemical companies.

2.2 Synthesis of PPy

Oxidant, $FeCl_3 \cdot 6H_2O$ (0.345mol) was dissolved in 100 ml distilled water in a reaction vessel under magnetic stirring. 0.15 mol freshly distilled pyrrole monomer was first dispersed in 50 ml of distilled water and

then added dropwise to the oxidant solution with stirring. Polymerization was carried out for 4 hr at room temperature by using a mechanical stirrer at moderate stirring speed (800 rpm). The precipitate was filtered off and washed with distilled water. The final black PPy powder was obtained after drying at 60 °C for 8 hr under reduced pressure.

2.3 Synthesis of PPy in the Presence of a Surfactant

$FeCl_3 \cdot 6H_2O$ (0.345 mol) or $Fe_2(SO_4)_3$ (0.18 mol) dissolved in 100 ml distilled water was mixed with a solution prepared by dissolving of 0.03 mol DBSNa in 100 ml distilled water and stirred for 15 min. Pyrrole was inserted to this mixture as 0.15 mol dispersed in 50 ml of distilled water drop by drop. Polymerization was carried out for 4 hr at room temperature by using a mechanical stirrer at moderate stirring speed (800 rpm). The work-up procedure was the same as described in section 2.2.

2.4 Preparation of PPy/MMT Nanocomposites

PPy/MMT nanocomposites with different amounts of MMT were prepared by two emulsion polymerization methods (A and B). The general procedure is given below. In the method (A), a water solution containing different amounts of oxidants ($FeCl_3 \cdot 6H_2O$ or $Fe_2(SO_4)_3$) and surfactant (DBSNa) was introduced to a suspension of MMT. In order to better dispersion, the final mixture was stirred for 1 h by using a high speed mechanical homogenizer. Pyrrole monomer dispersed in 50 ml distilled water was introduced dropwise while stirring and polymerization was then carried out at room temperature for 4 h. In the method (B), appropriate amount of pyrrole was added first to the suspension solution of MMT in distilled water. After 1 h stirring by using the high speed mechanical homogenizer, mixture of surfactant (DBSNa) and oxidizing agent dissolved in 100 ml distilled water was added to start polymerization. Polymerization reaction was continued for 4 h at room temperature. The products in the form of black powder were collected over a filter paper, washed several times with distilled water and vacuum dried at 60 °C for 24 h. Tbale 1 shows the encoding system for the compounds prepared and the amount of materials used in the preparation of them.

2.5 Characterization

Wide-angle X-Ray diffraction (WAXD) patterns were obtained by using a SIMENS D5000 diffractometer with Cu-Kα radiation by $\lambda = 0.154178$ nm at 40 kV and 30 mA. WAXD scans were performed at ambient temperature with a 2θ range between 2 and 10°, at a scanning rate of 0.04°/min.

The morphology of the synthesized PPy and nanocomposites was studied by scanning electron microscopy (SEM) using an OXFORD-LEO-440i scanning electron microscope. TEM images were taken by using a PHILIPS CM-200 FEG TEM at 200 kV acceleration voltages. Samples were prepared by putting powdered nanocomposites into epoxy resin capsules, followed by curing the epoxy resin at 100 °C for 24 h in a vacuum oven. Subsequently, the cured epoxy resin containing nanocomposites were ultramicrotomed with an ultramicrotome into 60 to 90 nm thick slices. The slices were then transferred on the surface of a 100-mesh copper grid for TEM observation.

Differential scanning calorimetry (DSC) analysis were carried out on a SHIMADZU DSC-60 differential scanning calorimeter under oxygen atmosphere at heating rate of 5 °C/min between 30 and 500 °C.

Thermogravimetric analysis (TGA) were performed by using a Perkin Elmer, Pyris Diamond TGA/DTA analyzer at a heating rate of 20 °C/min from room temperature up to 600 °C under nitrogen atmosphere.

Electrical measurements were carried out on disk shaped test prepared by compression molding of the materials between two Ni foils by a laboratory press. The dimensions of the disks were 16 mm in

diameter and 2 mm in overall thickness (each Ni foil was 0.1 mm in thickness). PPy/MMT test samples were prepared by applying 10 MPa mold pressure at room temperature. Two copper wires were soldered on each Ni foils and electrical measurements were carried out after 24 h relaxation time. Measurements were carried out on-line by using a digital multimeter (Keader® LDM-852A) or a LCR-meter (Escort® ELC-13C-131D) while the test samples were immersed in a silicon oil bath. The measured electrical resistivities were converted into specific resistivity (ρ) by using simple geometric calculations.

3. Results and Discussion

3.1 Synthesis of PPy

PPy samples have been prepared with and without using anionic surfactant in this work to investigate the effect of the surfactant on the properties of the synthesized PPy. The results were in general agreement to the previously published reports[9,27–29] however, only the morphological features and electrical properties are discussed in this paper.

Fig. 1 compares particle morphology for the PPy samples synthesized with and without using the anionic surfactant DBSNa. Fig. 1a shows the SEM micrograph for PPy-Cl synthesized without using DBSNa and Fig. 1b is the SEM micrograph for PPy-Cl-DBSNa sample prepared by the method described in section 2.3 in the presence of DBSNa. It is clear that particle morphology is different between these two types of PPy samples. They are in denser state in Fig. 1b in comparison to coral shape particles in Fig. 1a. This is happened because the reaction locus changes due to the presence of the surfactant in the reaction mixture. Particle density plays an important role in the electrical conductivity of the substantially conductive polymeric materials which is discussed in latter sections in this paper.

3.2 Preparation of PPy/MMT

PPy/MMT nanocomposites were prepared by two emulsion polymerization methods (A and B). According to the procedure provided in section 2.4, several types of PPy/MMT nanocomposites were prepared by using different amounts of constituents as is summarized in Table 1.

So far, PPy/MMT nanocomposites have been synthesized by several methods and using several starting materials. Recently, emulsion[57] and reverse emulsion[8,54] methods were employed mostly by using DBSA as the surfactant. Several types of oxidants including ammonium persulfate and $FeCl_3$ were the employed oxidant in those methods. Different reaction times from 1h to 40h, and temperatures from 5 °C up to room temperatures also were applied for the synthesis of PPY/MMT nanocomposites. Organically modified MMT and

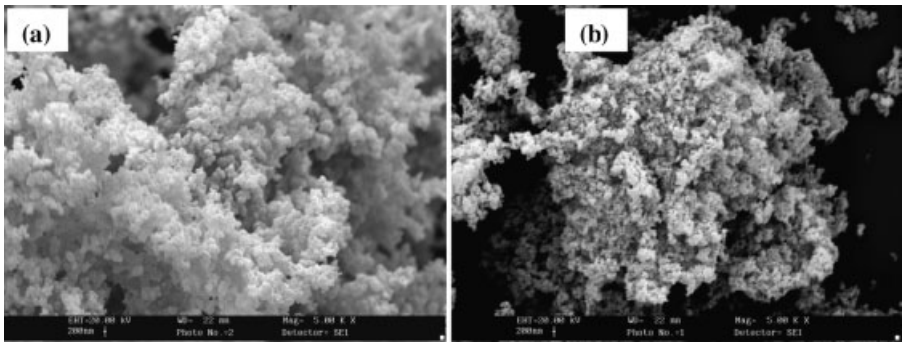

Figure 1.
SEM images for PPy-Cl (a) and PPy-Cl-DBSNa (b).

Table 1.
Encoding system and amounts of materials used for the preparation of the compounds described in section 2.2, 2.3 and 2.4.

Material	Mole of monomer	Mole of oxidant	Mole of surfactant	Montmorillonite Percent	Polymerization procedure
PPy-Cl	0.15	0.345	–	–	2.2
PPy-Cl-DBSNa	0.15	0.345	0.03	–	2.3
PPy-SO_4-DBSNa	0.15	0.18	0.03	–	2.3
PPy-Cl(A)/MMT(15)	0.15	0.345	0.03	15	2.4 (A)
PPy-Cl(B)/MMT(15)	0.15	0.345	0.03	15	2.4 (B)
PPy-SO_4(B)/MMT(14)	0.15	0.18	0.03	14	2.4 (B)
PPy-SO_4(B)/MMT(17.5)	0.15	0.18	0.03	17.5	2.4 (B)
PPy-SO_4(B)/MMT(24)	0.15	0.18	0.03	24	2.4 (B)

Na-MMT was the chosen clay in different methods of the syntheses. In this work, PPy/MMT samples were prepared thoroughly in water using DBSNa at room temperature in 4h and using $FeCl_3$ or $FeSO_4$ as the oxidizing agent. The samples also were prepared by using unmodified Na-MMT. The main feature in the two synthetic methods (A and B) used in this work was the different sequence of addition of pyrrole monomer to the reaction mixture i.e. after addition of the oxidizing agent (method A) or before it (method B). Discussions of the results provided in the later sections will show the effect of this alternation in addition sequence of the monomer.

XRD studies revealed formation of the intercalated structure in the PPy/MMT nanocomposites. Fig. 2 shows the X-ray diffraction patterns for MMT, PPy-Cl(B)/MMT(15), PPy-Cl(A)/MMT(15), PPy-SO_4(B)/MMT(17.5) and PPy-SO_4(B)/MMT(24). The peak appeared at 5.9 on the 2θ axis in Fig. 2a is the diffraction peak from (001) planes in pristine MMT which is equal to 1.5 nm basal spacing according to the Bragg's law. As can be seen, for the PPy/MMT nanocomposites, peaks due to (001) planes are shifted toward lower 2θ

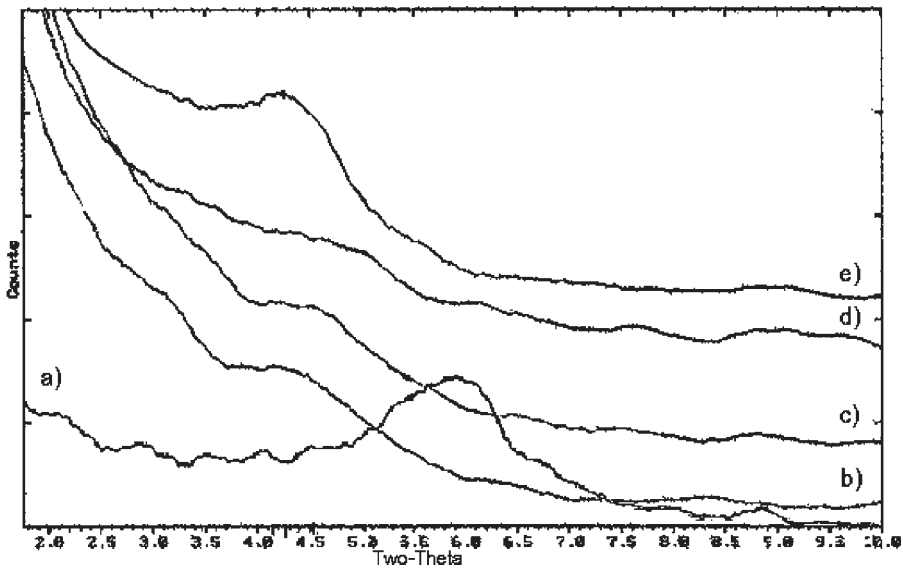

Figure 2.
XRD patterns for a) MMT, b) PPy-SO_4(B)/MMT(24), c) PPy-SO_4(B)/MMT(17.5), d)) PPy-Cl(A)/MMT(15) and e) PPy-Cl(B)/MMT(15).

Table 2.
Basal spacing and diffraction angles from (001) clay planes in different types of PPy/MMT nanocomposites and MMT.

Curve	Nanocomposite Type	2θ (degree)	d_{001} (nm)
a	MMT	5.9	1.5
b	PPy-SO_4(B)/MMT(24)	4.15	2.13
c	PPy-SO_4(B)/MMT(17.5)	4.55	1.94
d	PPy-Cl(A)/MMT(15)	5	1.77
e	PPy-Cl(B)/MMT(15)	4.27	2.07

angles which means the increasing of basal spacing. From the obtained diffraction patterns, formation of the intercalated structure can be concluded for PPy/MMT nanocomposites. The numerical values for (001) diffraction angle and basal spacing of the clay layers are summarized in Table 2. The observed increase in basal spacing is ranging from 1.5 nm (for pristine MMT) up to 2.13 (for PPy-SO_4(B)/MMT(24). By comparison of data in Table 2 it can be concluded that the method B of preparation in which, the pyrrole monomer was added to the reaction mixture before polymerization, has leaded to higher basal spacing of the clay layers or more intercalation of PPy chains.

Fig. 3 shows the SEM micrographs for pristine MMT and as synthesized PPy-SO_4(B)/MMT(14) and PPy-SO_4(B)/MMT(24) nanocomposites. Fig. 3b and 3c shows that PPy is formed around the MMT particles and the coating area decreases as MMT amount increases in the nanocomposites. Therefore, in combination with the results obtained from XRD investigations, PPy chains are not only produced inside the clay gallery spaces but also on the surface of MMT particles. This may be due to the anionic characteristics of clay layers, which act as counter ion for oxidized cationic PPy chains.

Transmission electron microscopy images provided a proof for the formation of intercalated structure for PPy/MMT nanocomposites, in accordance to the results obtained by XRD studies. Fig. 4 shows TEM images for PPy-SO4(B)/MMT(14) in two magnification levels.

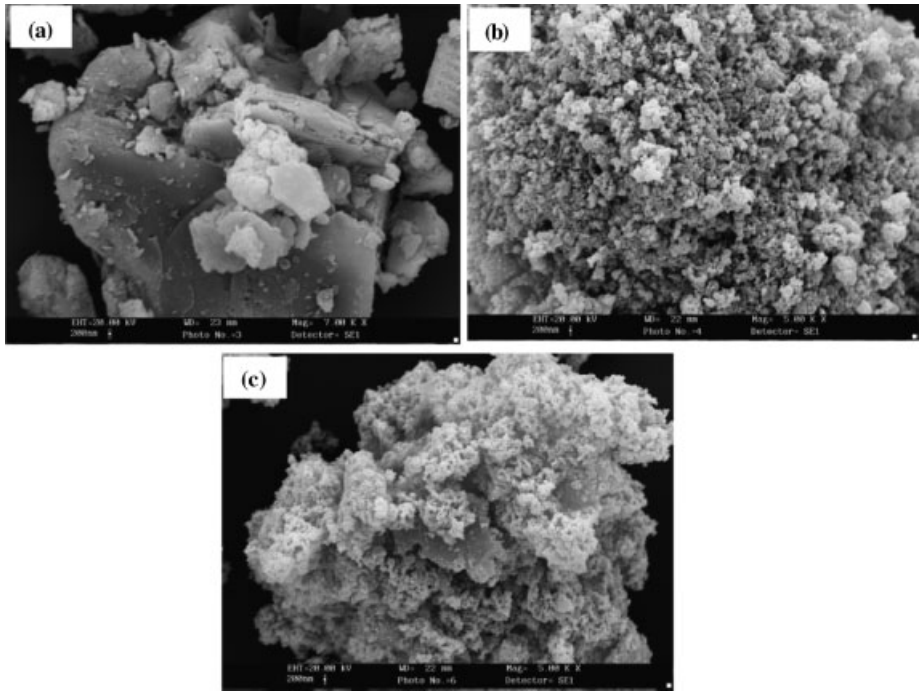

Figure 3.
SEM micrographs for (a) pristine MMT, (b) PPy-SO_4(B)/MMT(14) and (c) PPy-SO_4(B)/MMT(24) nanocomposites.

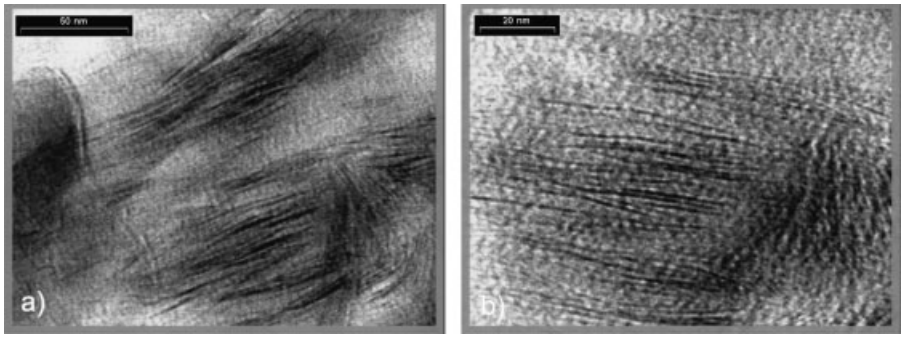

Figure 4.
TEM images for PPy-SO4(B)/MMT(17.5) in two magnification levels.

Stacking of MMT layers as black strips with thicknesses of about 1 nm and lengths of 40-50 nm are clear in the images which are distributed in the light background PPy matrix.

3.3 Electrical Conductivities at Room Temperature

The electrical resistivity (R) of the test samples, prepared as described in section 2.5 were measured at room temperature and then converted to volume specific resistivity (ρ) by using the equation: $R = \rho L/A$. In this equation, A is the test sample cross section area and L, the sample thickness. Finally, the electrical conductivity (σ) will be the reciprocal of ρ ($\sigma = 1/\rho$). Table 3 summarizes the results obtained for different types of PPy and PPy/MMT nanocomposites. As can be seen, ρ is decreased (σ is increased) almost 6 times for PPy-Cl-DBSNa in comparison to PPy-Cl. Higher densities acquired by the synthesis of PPy in the presence of surfactant, as discussed earlier based on SEM studies, may be the responsible factor for higher electrical conductivity observed for PPy-Cl-DBSNa. PPy chains contain various types of structural disorders which considerable influence the charge-carrier transport and finally the conductivity of the polymer. From the other hand and due to the fact that anionic surfactant also changes the locus of polymerization to proceed via the emulsion polymerization mechanism, there is a possibility to modify the chain regularity.[27] The highest conductivity in Table 3 is observed for the sample PPy-SO4-DBSNa. Therefore, the electrical resistivity is not only dependent to the synthesis protocol but also to the type of the oxidant used. The size of counter ion came from the oxidant and its concentration would be effective in the electrical conductivity of the doped conducting polymers.[29] In our syntheses, oxidant played two roles, as an initiator for oxidative polymerization pyrrole and as dopant. Therefore, counter ions from the oxidant remain between the chains as counter ion

Table 3.
Electrical properties of different types of PPy and PPy/MMT nanocomposites.

Material	Volume Specific Resistivity, ρ ($\Omega \cdot$ cm)	Electrical Conductivity, σ (S/cm)
PPy-Cl	680.77	0.0015
PPy-Cl-DBSNa	110.21	0.0091
PPy-SO_4-DBSNa	38.962	0.0257
PPy-Cl(A)/MMT (15)	1091.5	$9.162^{*}10^{-4}$
PPy-Cl(B)/MMT (15)	775.6	$1.289^{*}10^{-3}$
PPy-SO_4(B)/MMT (14)	993.1	$1.007^{*}10^{-3}$
PPy-SO_4(B)/MMT (17.5)	1022.6	$9.78^{*}10^{-4}$
PPy-SO_4(B)/MMT (24)	2704.3	$3.68^{*}10^{-4}$

for the cationic charge-carriers. The oxidant/monomer ratio was 1.2 for the case of $Fe_2(SO_4)_3$ and 2.3 for $FeCl_3$ (Table 1) in the synthesis of PPy samples. Therefore, lower concentration of counter ions would be the responsible factor for higher conductivity of the sample PPy-SO_4-DBSNa.

In Table 3, specific resistivity ρ, increases with MMT content between PPy/MMT nanocomposites. This is a predictable result because clays like montmorillonite are substantially electrically insulator compounds. The penetrated clay layers prevent the charge carrier motions and then cause weak chain interactions which in turn results a decreased electrical conductivity. Electrical resistivity also depends on the applied preparation method of PPy/MMT nanocomposites. This amount is 1091.5(Ω · cm) for PPy-Cl(A)/MMT(15) and 775.6 (Ω · cm) for PPy-Cl(B)/MMT(15). Therefore, polymerization method B resulted in lower electrical resistivity for PPy/MMT nanocomposites. The reason of this phenomenon can be justified in terms of more polymeric chains intercalated between the clay gallery spaces, as is confirmed by XRD studies in section 3.1. In the method B, pyrrole monomer was mixed with the clay suspension before polymerization has started. This let monomers to intercalate between the clay layers and form PPy chains upon subsequent in-situ polymerization. Therefore, more intercalation of the chains leads to more effective interchain interactions and more continuity in conduction network in the composite.

3.4 Thermal Properties of the Nanocomposites

Thermogravimetric analysis (TGA) of the samples has been performed under N_2 atmosphere between room temperature up to 600 °C. The results are shown in Fig. 5. Below 100 °C there is not any significant weight loss for none of the samples which indicates absence of water adsorbed by the samples. Between 100 and 300 °C, a weight loss of about 5% can be seen for all of the samples while this amount is seen to be slightly higher (higher weight loss) for the nanocomposites which may be attributed to the unreacted pyrrole mono-

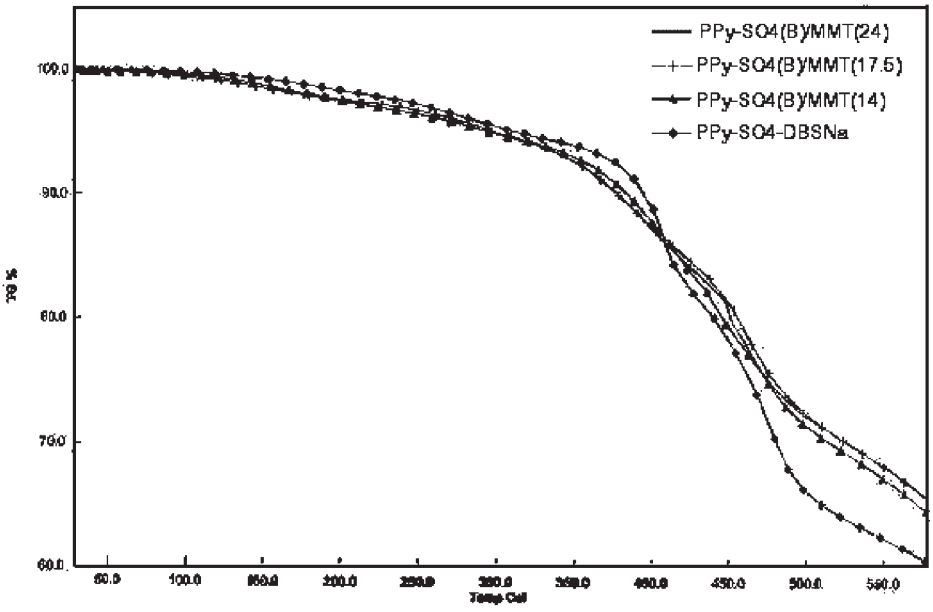

Figure 5.
TGA results for PPy-SO4-DBSNa and different PPy/MMT samples under N_2 atmosphere and 20 °C/min heating rate.

mers entrapped between the clay layers. The principal weight loss peak starts at 305 °C. This is in consistence with the results obtained by J.M Yeh and co-workers[57] which incorporation of clay layers lead to an insignificant increase in initial decomposition temperature of PPy/MMT nanocomposites. After this temperature, PPy-SO_4-DBSNa shows a fast decomposition behavior while the rate of decomposition is slower for PPy/MMT nanocomposites as temperature increases. This can be mentioned as the main effect of the added clay in the thermal stability of the resulting nanocomposites. The effect is attributed to the decomposition retardation effect of the clay layers in the nanocomposites series. From the other hand the weight loss for PPy-SO_4-DBSNa at 600 °C is 40% however; this value is smaller for the nanocomposites and around 33%. This is obviously due to the minerals remained after complete decomposition of the PPy matrix in the nanocomposites. Between the nanocomposites, it can be seen that there is not any significant differences between PPy-SO_4(B)/MMT(17.5) and PPy-SO_4(B)/MMT(24). In fact, in polymer/clay nanocomposites, physical and mechanical properties of the nanocomposites, including the thermal properties, do not vary with increasing the clay content after some loading level of the filler.[47] As an overall result, the neat effect of the clay layers is to reduce the thermal decomposition rate of PPy chains intercalated between the clay layers and to increase the residual weigh after complete thermal decomposition of the PPy.

Fig. 6 represents the results obtained by DSC studies performed on the samples PPy-SO_4-DBSNa and PPy-SO_4(B)/MMT(24) under oxygen atmosphere between room temperature and 500 °C. This study showed glass-transition temperature T_g, at 105 °C for PPy-SO_4-DBSNa in agreement to the previously reported value.[57] This value has increased to 115 °C for the sample PPy-SO_4(B)/MMT(24). Increase in T_g is a known behavior in polymer/clay nanocomposites and has been reported for several types of polymer/clay nanocomposites.[57] The reason can be attributed to the polymer-clay layer interactions, which restrict segmental chain motions around T_g of the polymeric matrix.

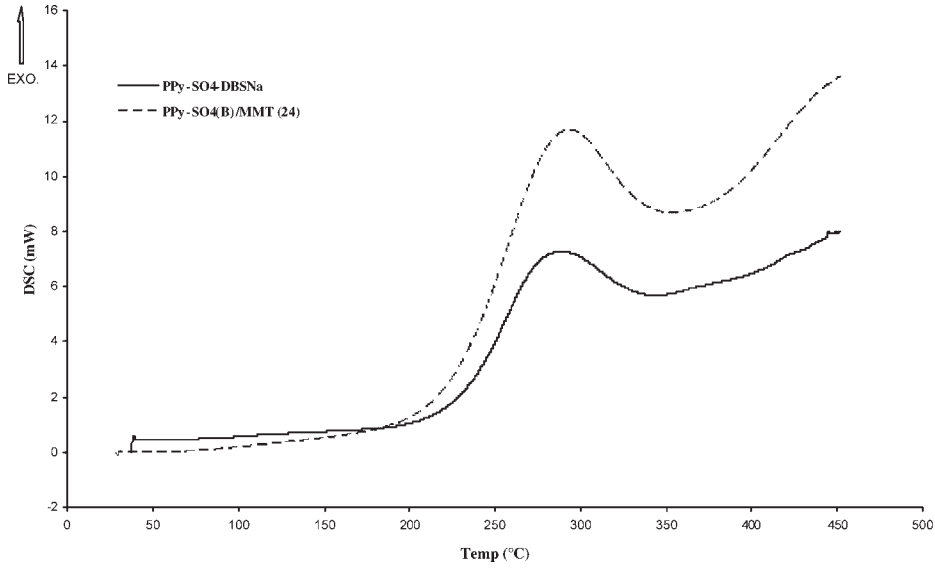

Figure 6.
DSC curves for PPy-SO_4-DBSNa and PPy-SO_4(B)/MMT(24), under oxygen atmosphere and heating rate of 5 °C/min.

As can be seen in Fig. 6, an exothermic peak.

Which commences at 230 °C and ends at 330 °C, arise for PPy-SO4-DBSNa. This shows that decomposition has occurred before the sample melt. A similar decomposition peak also is observed for the sample PPy-SO_4(B)/MMT. It commences at the same temperature as PPy-SO4-DBSNa however, ends at higher temperatures around 350 °C. This is the effect of clay layers in diminishing the decomposition rate of the polymer matrix as is discussed for TGA results.

4. Conclusion

Electrically conductive PPy/MMT nanocomposites synthesized in this work by a one-pot emulsion polymerization of pyrrole monomer in the presence of unmodified montmorillonite and using DBSNa as the surfactant. XRD and TEM studies showed the existence of intercalated structures for the PPy/MMT nanocomposites prepared by this method. Electrical conductivity measurements were carried out on the test samples in which conducting materials were sandwiched between two Ni electrodes. Electrical conductivity of the nanocomposites measured to be in the range of 1.00×10^{-3} and 3.68×10^{-4} (S/cm) depending on the clay content and method of polymerization. Higher electrical conductivity was achieved for the nanocomposites in a same level of clay loading by oxidative polymerization of previously intercalated pyrrole monomers between the clay layers (method B of synthesis in this work). Electrical conductivity of the samples verified to be dependent to the oxidant type and molar ratio of oxidant to monomer. Investigation of thermal properties showed a higher thermal stability for PPy/MMT nanocomposites in comparison to PPy itself as one of the superior properties came with polymer/clay nanocomposite systems.

Acknowledgements: The authors wish to express their gratitude from the research department of the Sahand University of Technology for its financial supports of the current work.

[1] S. Chao, M. S. Wrighton, *J. Am. Chem. Soc.* **1987**, *109*, 2197.
[2] L. W. Shacklette, R. R. Chance, D. M. Ivory, G. G. Miller, R. H. Baughman, *Synth. Met.* **1979**, *1*, 101.
[3] L. H. M. Krings, E. E. Havinga, J. J. T. M. Donkers, *Synth. Met.* **1993**, *54*, 453.
[4] Y. Z. Wang, D. D. Gebler, L. B. Lin, J. W. Blatchford, S. W. Jessen, H. L. Wang, A. J. Epstein, *Appl. Phys. Lett.* **1996**, *68*, 894.
[5] J. Joo, C. Y. Lee, *J. Appl. Phys.* **2000**, *88*, 513.
[6] M. D. Imisides, R. John, P. J. Reiley, G. G. Wallace, *Electroanalysis* **1991**, *3*, 879.
[7] T. Lindfors, J. Bobacka, A. Lewen Stam, A. Ivaska, *Electrochim. Acta* **1998**, *43*, 3503.
[8] S. H. Hong, B. H. Kim, J. Joo, J. W. Kim, H. J. Choi, *Current Appl. Phys.* **2001**, *1*, 447.
[9] M. Omastová, M. Trchová, J. Kovářová, J. Stejskal, *Synth. Mel.*, **2003**, *138*, 447.
[10] A. F. Diaz, K. K. Kanazawa, G. P. Gardini, *J. Chem. Soc., Chem. Commun.* **1979**, 635.
[11] A. F. Diaz, J. Bargon, in: *Handbook of Conducting Polymers*, T.A. Skotheim (Ed.), Vol. *1*, Marcel-Dekker, New York **1986**, P. 82.
[12] J. Ouyang, Y. Li, *Polymer* **1997**, *38*, 3997.
[13] R. E. Myers, *J. Electron. Mater.* **1986**, *15*, 61.
[14] S. P. Armes, *Synth. Met.* **1987**, *20*, 365.
[15] J. C. Thieblemont, A. Brun, J. Marty, M. F. Planche, P. Calo, *Polymer* **1995**, *36*, 1605.
[16] K. Nishino, M. Fujimoto, O. Ando, H. Ono, T. Murayama, *J. Appl. Electrochem.* **1996**, *26*, 425.
[17] C. Cassignol, P. Olivier, A. Ricard, *J. Appl. Polym. Sci.* **1998**, *70*, 1557.
[18] E. J. Oh, K. S. Jang, A. G. MacDiarmid, *Synth. Met.* **2002**, *125*, 267.
[19] C. DeArmitt, S. P. Armes, *Langmuir* **1993**, *9*, 652.
[20] S. Y. Luk, W. Lineton, M. Keane, C. DeArmitt, S. P. Armes, *J. Chem. Soc. Faraday Trans.* **1995**, *91*, 905.
[21] J. Stejskal, *J. Polym. Mater.* **2001**, *18*, 225.
[22] P. J. Kinlen, J. Liu, Y. Ding, C. R. Graham, E. E. Remsen, *Macromolecules* **1998**, *31*, 1735.
[23] S. Palaniappan, *Polym. Adv. Technol.* **2002**, *13*, 54.
[24] H. Xia, Q. Wang, *J. Nanoparticle Res.* **2001**, *3*, 401.
[25] P. S. Rao, S. Subrahmanya, D. N. Sathyanarayana, *Synth. Met.* **2002**, *128*, 311.
[26] P.S. Rao, D. N. Sathyanarayana, S. Palaniappan, *Macromolecules* **2002**, *35*, 4988.
[27] J. Stejskal, M. Omastová, S. Fedorova, J. Prokeš, M. Trchová, *Polymer* **2003**, *44*, 1353.
[28] M. Omastová, J. Pionteck, M. Trchová, *Synth. Met.* **2003**, *135-136*, 437.
[29] G. J. Lee, S. H. Lee, K. S. Ahn, K. H. Kim, *J. Appl. Polym. Sci.* **2002**, *84*, 2583.
[30] I. W. Kim, J. Y. Lee, H. Lee, *Synth. Met.* **1996**, *78*, 177.
[31] N. Gospodinova, P. Mokreva, T. Tsanov, L. Terlemezyan, *Polymer* **1997**, *38*, 743.

[32] Y. H. Lee, J. Y. Lee, D. S. Lee, *Synth. Met.* **2000**, *114*, 347.
[33] E. Segal, O. Aviel, M. Narkis, *Polym. Eng. Sci.* **2000**, *40*, 1915.
[34] M. Narkis, Y. Haba, E. Segal, M. Zilberman, G. Titelman, A. Siegmann, *Polym. Adv. Technol.* **2000**, *11*, 665.
[35] J. Stejskal, *J. Polym. Mater.* **2001**, *8*, 225.
[36] M. G. Han, S. K. Cho, S. G. Oh, S. S. Im, *Synth. Met.* **2002**, *126*, 53.
[37] Y. Shen, M. Wan, *Synth. Met.* **1998**, *96*, 127.
[38] P. J. Kinlen, B. G. Frushour, Y. Ding, V. Menon, *Synth. Met.* **1999**, *101*, 758.
[39] M. Wan, J. Huang, Y. Shen, *Synth. Met.* **1999**, *101*, 708.
[40] M. Wan, J. Li, S. Li, *Polym. Adv. Technol.* **2001**, *12*, 651.
[41] A. J. Dominis, G. M. Spinks, L. A. P. Kane-Maguire, G. G. Wallace, *Synth. Met.* **2002**, *129*, 165.
[42] Y. Kudoh, *Synth. Met.* **1996**, *79*, 17.
[43] M. T. Gill, S. E. Chapman, C. L. DeArmitt, F. L. Baines, C. M. Dadswell, J. G. Stamper, G. A. Lawless, N. C. Billingham, S. P. Armes, *Synth. Met.* **1998**, *93*, 227.
[44] R. Turcu, L. V. Giurgiu, R. Ordean, Grecu M. Brie, *Synth. Met.* **2001**, *119*, 287.
[45] L. Bay, K. West, S. Skaarup, *Polymer* **2002**, *43*, 3527.
[46] Z. Zhang, Z. Wei, M. Wan, *Macromolecules* **2002**, *35*, 5937.
[47] S. S. Ray, M. Okamoto , *Prog. Polym. Sci.* **2003**, *28*, 1539.
[48] T. Agag, T. Takeichi, *Polymer* **2000**, *41*, 7083.
[49] J.W. Gilman, R. Harris, D. Hunter, in: 44th International SAMPE Symposium/Exihibition, **1999**, P. 1408.
[50] J. W. Kim, F. Liu, H. J. Chio, S. H. Hong, J. Joo, *Polymer* **2003**, *44*, 289.
[51] D. P. Park, J. W. Kim, F. Liu, H. J. Choim, and J. Joo, *Synth. Met.* **2003**, *135-136*, 713.
[52] Y. C. Liu, M. D. Ger, *Chem. Phys. Lett.* **2002**, *362*, 491.
[53] S. Yoshimoto, F. Ohashi, T. Kameyama, *Macromol. Rapid Commun.* **2005**, *26*, 461.
[54] B. H. Kim, S. H. Hong, J. W. Kim, H. J. Choi, J. Joo, *Synth. Met.* **2003**, *135-136*, 771.
[55] S. S. Ray, *Mater. Res. Bull.* **2002**, *37*, 813.
[56] *Intercalation Chem.*, M. S. Whittingham, Ed., Academic Press, New York **1982**.
[57] J. M. Yeh, C. P. Chin, S. Chang, *J. Appl. Polym. Sci.* **2003**, *88*, 3264.

